Optics Communications 284 (2011) 1603–1607

Contents lists available at ScienceDirect

Optics Communications

journal homepage: www.elsevier.com/locate/optcom

Double dark resonances and the dispersion properties in a four-level inverted-Y atomic system

Jun Kou [a,b], Ren-Gang Wan [a,b], Shang-Qi Kuang [a,b,c], Li Jiang [a,b], Liang Zhang [a,b], Zhi-Hui Kang [a,b], Hai-Hua Wang [a,b], Jin-Yue Gao [a,b,*]

[a] College of Physics, Jilin University, Changchun 130000, China
[b] Key Laboratory of Coherent Light and Atomic and Molecular Spectroscopy of Ministry of Education, Jilin University, Changchun 130000, China
[c] Changchun Institute of Optics, Fine Mechanics and Physics, Chinese Academy of Sciences, Changchun 130033, China

ARTICLE INFO

Article history:
Received 19 August 2010
Received in revised form 1 November 2010
Accepted 20 November 2010

Keywords:
Electromagnetically induced transparency
Double dark resonances
Atomic coherence

ABSTRACT

The electromagnetically induced transparency (EIT) and its dispersion properties in a four-level inverted-Y atomic system are investigated. The absorption spectrum of a weak probe field shows two EIT windows (dark resonances) whose location, width, and depth can be controlled by manipulating the parameters of the coupling fields; the corresponding dispersion properties are also measured by using a Mach–Zehnder interferometer. The experimental measurements agree well with the theoretical calculations. This kind of system can find important applications in two-channel quantum communication and information storage.

1. Introduction

Electromagnetically induced transparency (EIT) refers to the phenomenon that an otherwise opaque medium on a probe resonance is made highly transparent, such spectral feature, often called dark resonance, arises from the destructive interference between two possible excitation paths [1]. Light manipulation techniques based on EIT are of importance in various fields of physics, such as controlling the group velocity of a pulsed probe field [2,3], quantum information storage [4–6], and enhancement of frequency conversion [7,8].

When an additional resonant transition, driven by an optical [9–14] or microwave (or radio-frequency) field [15–17], is added to the three-level system, a double dark resonance can occur. In the past few years, many new EIT-related effects in a variety of four-level systems have been investigated. A photon switching by quantum interference in a four-level *N*-type EIT system has been theoretically proposed by Harris and Yamamoto [18] and experimentally demonstrated in cold atoms by Yan et al. [19]. Sharypov and Wilson-Gordon discussed sub-Doppler features due to double dark resonances in atomic vapor [20]. Li et al. used a tripod-type system to achieve enhanced cross-phase modulation based on a double EIT [21].

Recently, some novel effects based on EIT in a four-level inverted-Y system have been extensively studied [22–27]. In theory, it has been shown that four-level inverted-Y EIT system can be adopted to generate a polarization quantum phase gates [23], realize two-channel quantum memory [24], obtain nonclassical paired photons [25], and produce optical solitons [26,27]. In experiment, Yan et al. showed the suppression of two-photon absorption owing to quantum interference [28], and Mohapatra et al. implemented the coherent optical detection of highly excited Rydberg states [29]. It is necessary to further explore the EIT characteristics experimentally in the four-level inverted-Y system. In this paper, we focus on the theoretical calculations and experimental observations of two EIT windows (double dark resonances) and the corresponding dispersion properties in a four-level inverted-Y atomic system.

2. Theoretical basis

The relevant atomic levels in ^{87}Rb atoms are depicted in Fig. 1. The probe field Ω_p couples the transition $|1\rangle(5S_{1/2}, F=1)\rightarrow|3\rangle(5P_{1/2}, F=2)$, and two coupling fields Ω_{c1} and Ω_{c2} are tuned to the transition $|2\rangle(5S_{1/2}, F=2)\rightarrow|3\rangle$and the transition $|3\rangle\rightarrow|4\rangle(5D_{3/2}, F=3)$, respectively. $\Delta_p=\omega_p-\omega_{31}$, $\Delta_{C1}=\omega_{C1}-\omega_{32}$ and $\Delta_{C2}=\omega_{C2}-\omega_{43}$ represent the respective single-photon detunings, and $\omega_{ij}=\omega_i-\omega_j$ is the transition frequency corresponding to the level$|i\rangle\rightarrow|j\rangle$ ($i, j=1, 2, 3, 4$).

* Corresponding author.
E-mail address: jygao@mail.jlu.edu.cn (J.-Y. Gao).

0030-4018/$ – see front matter © 2010 Elsevier B.V. All rights reserved.
doi:10.1016/j.optcom.2010.11.061

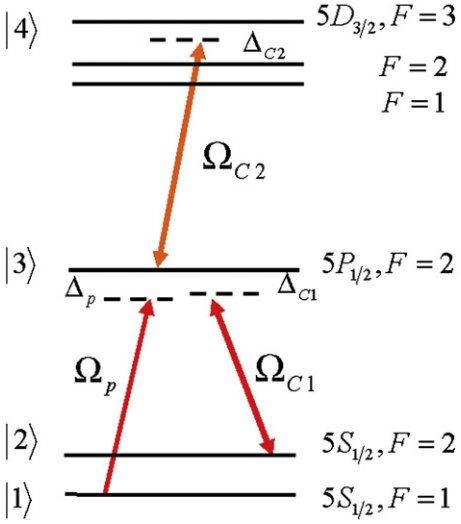

Fig. 1. Relevant energy levels of ^{87}Rb atoms and laser excitations in the experiment.

In the interaction picture, with the rotating-wave and electric-dipole approximations, the Hamiltonian can be expressed as

$$H = \hbar\left(\Delta_p - \Delta_{C1}\right)|2\rangle\langle 2| + \hbar\Delta_p|3\rangle\langle 3| + \hbar\left(\Delta_p + \Delta_{C2}\right)|4\rangle\langle 4| - \hbar\left[\Omega_p|3\rangle\langle 1| + \Omega_{C1}|3\rangle\langle 2| + \Omega_{C2}|4\rangle\langle 3| + h.c.\right] \quad (1)$$

Solving the Liouville equation $\frac{\partial\rho}{\partial t} = -\frac{i}{\hbar}[H,\rho] - \frac{1}{2}\{\Gamma,\rho\}$, one obtains

$$\rho_{13} = \frac{\Omega_p}{\Delta_p + i\gamma_{13} - \frac{\Omega_{C1}^2}{\Delta_p - \Delta_{C1} + i\gamma_{12}} - \frac{\Omega_{C2}^2}{\Delta_p + \Delta_{C2} + i\gamma_{14}}} \quad (2)$$

The coherent decay rates are denoted as $\gamma_{12}=\Gamma_{21}/2, \gamma_{13}=\gamma_{23}=(\Gamma_{31}+\Gamma_{32})/2$, $\gamma_{14}=\gamma_{24}=\Gamma_{43}/2$, $\gamma_{34}=(\Gamma_{43}+\Gamma_{32}+\Gamma_{31})/2$. Here $\Gamma_{ij}(i, j=1,2,3,4)$ refers to the spontaneous decay rate of the populations from level $|i\rangle$to level$|j\rangle$.

Considering the frequency shift caused by the Doppler effect, for the moving atoms with velocity v, the frequency detunings of the probe, coupling and control fields are revised to $\Delta_p + \omega_p\frac{v}{c}, \Delta_C + \omega_{C1}\frac{v}{c}$ and $\Delta_k - \omega_{C2}\frac{v}{c}$, respectively. The susceptibility of the probe field is given by

$$\chi = \frac{|\mu_{31}|^2}{\hbar\varepsilon_0\Omega_p}\int_{-\infty}^{+\infty}\rho_{13}N(v)dv \quad (3)$$

where μ_{31} is the dipole matrix element of the probe transition, and $N(v) = \frac{N_0}{u\sqrt{\pi}}e^{-v^2/u^2}$is the Maxwellian velocity distribution, $u/\sqrt{2}$ is the root-mean-square atomic velocity, depending on the temperature of the cell, and N_0 is the total atomic density of the vapor. The real and imaginary part of χ represent the dispersion and absorption properties of the probe transition, respectively.

In such scheme, the existence of double dark resonances induces two EIT windows whose location, width, and depth can be controlled by manipulating the parameters of the coupling fields. By adjusting the detunings of the two coupling fields, it is possible to obtain two separate EIT windows or one enhanced EIT window, companied with corresponding dispersion properties. The group velocity in two EIT channels can be controlled independently by adjusting the intensity of the coupling fields, respectively. Therefore, the EIT characteristics in the inverted-Y system can provide effective method for two-channel quantum communication and information storage.

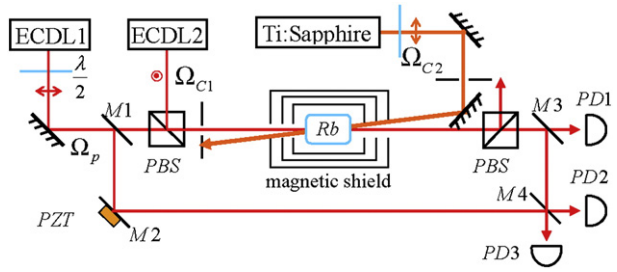

Fig. 2. Schematic of the experimental setup, where λ/2: half-wave plate; PBS: polarizing beam splitter; PD: photodiode; M: reflecting mirror; PZT: piezoelectric transducer.

3. Experimental setup and results

The experimental setup in this work is shown in Fig. 2. An extended-cavity diode laser tuned to the |2>→|3>transition at 795 nm serves as the coupling field Ω_{C1}. Another extended-cavity diode laser at 795 nm is used as the weak probe field Ωp and scans across the |1>→|3>transition. A Ti:Sapphire laser at 762 nm is used as the second coupling field Ω_{C2} and is tuned to the |3>→|4>transitions. The second coupling field Ω_{C2} propagates opposite to the probe field Ω_p and the coupling field Ω_{C1} with an angle of about 0.01 rad. Beam diameters of the probe and two coupling fields are about 1, 2, 3 mm, respectively. A photodiode (PD1) measures absorption of the probe laser passing through the atomic vapor cell. A 5-cm-long Rb vapor cell is kept at 30 °C (corresponding to atomic density of ~10^{10} cm^{-3}) and installed in a three-layer magnetic shield.

The dispersion properties of the coherent prepared atomic medium are measured by using a Mach–Zehnder interferometer [30] consisting of M_1, M_2, M_3 and M_4, and the differential signal of the detectors PD2 and PD3 is given by

$$\Delta I_d(\omega) \propto 2|E_R||E_P|\ exp(-\alpha(\omega)L/2)\ cos\left(\phi_0 + k_p n(\omega)L\right) \quad (4)$$

where E_p is the probe field passing through the cell and E_R is the reference field through the other arm. $\alpha(\omega)$ is the absorption coefficient, L is the length of the rubidium cell, and ϕ_0 is the reference phase of the interferometer, which is reset to $\pi/2$ by a piezoelectric transducer (PZT).

It can be considered that the inverted-Y system consists of two different EIT sub-systems, levels|1>, |2>and |3>are in a three-level Λ-type system, while levels |1>, |3>and |4>form a three-level ladder-type system. We first concentrate on the situation when both the coupling fields are on resonance, i.e., $\Delta_{C1}=\Delta_{C2}=0$ MHz. The plots of absorption as a function of probe detuning are shown in Fig. 3. Curve (a), (b) and (c) are for the coupling field Ω_{C2} is kept with the powers of 50 mW, while the coupling field Ω_{C1} is applied with the powers of 0, 3 and 10 mW, respectively. Curve (f), (g) and (h) depict the dispersion properties of EIT. On the other hand, Fig. 3(c), (d) and (e) represent the absorption properties when the coupling field Ω_{C1} is kept with the powers of 10 mW, while coupling field Ω_{C2} is applied with the powers of 50, 100 and 0 mW, respectively. The corresponding dispersion properties are plotted in (h), (i) and (g). The combined effects of these two sub-systems (the Λ-sub-system and the ladder-sub-system) can be seen in Fig. 3 (c) and (h) where we keep two coupling fields both existing, which show the depth of the EIT window and dispersion increase observably, the total depth increases to about 1.3 times of the single EIT window depth (Fig. 3 (e)), the enhancement of EIT window and dispersion can be owed to the interaction of two dark resonances.

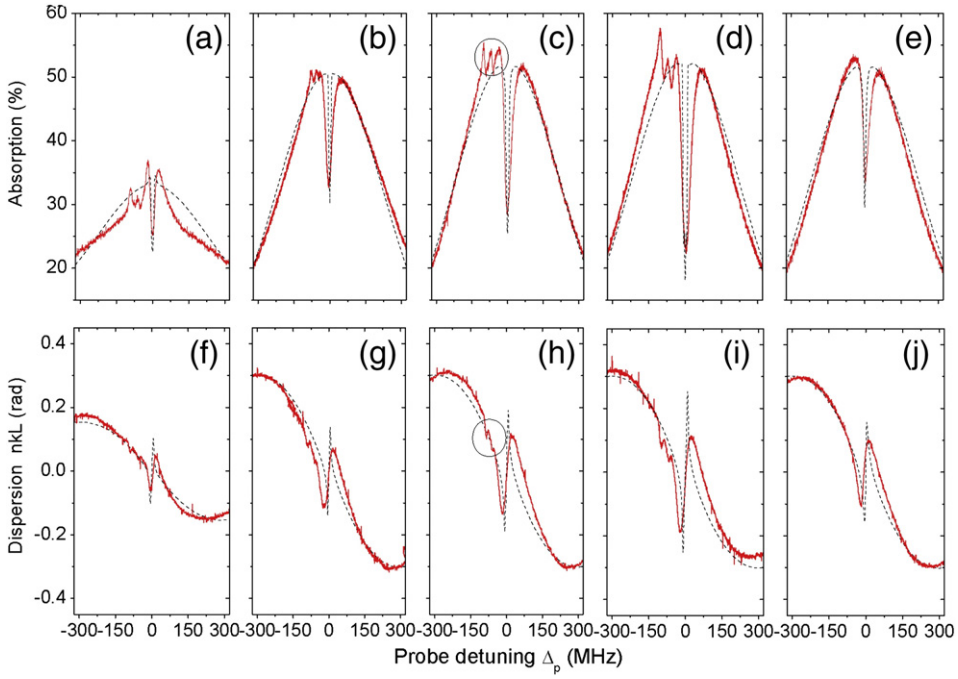

Fig. 3. Red solid curves, experimental measured absorption [(a)–(e)] and the corresponding dispersion [(f)–(j)] as a function of probe detuning Δ_p. Black dashed curves, theoretical predictions calculated at $\Gamma_{31}=\Gamma_{32}=3.0$ MHz, $\Gamma_{43}=0.4$ MHz, (a) $\Omega_{C1}=0$ MHz, $\Omega_{C2}=15$ MHz; (b) $\Omega_{C1}=15$ MHz, $\Omega_{C2}=15$ MHz; (c) $\Omega_{C1}=30$ MHz, $\Omega_{C2}=15$ MHz; (d) $\Omega_{C1}=30$ MHz, $\Omega_{C2}=20$ MHz; (e) $\Omega_{C1}=30$ MHz, $\Omega_{C2}=0$ MHz.

The dark state in the inverted-Y atomic system can be analyzed by using the method discussed in [31], and there are three dark states (noncoupled states) which can be expressed as $|D_1\rangle = \frac{\Omega_{C1}}{\sqrt{\Omega_p^2+\Omega_{C1}^2}}|1\rangle + \frac{\Omega_p}{\sqrt{\Omega_p^2+\Omega_{C1}^2}}|2\rangle$, $|D_2\rangle = \frac{\Omega_{C2}}{\sqrt{\Omega_p^2+\Omega_{C2}^2}}|1\rangle + \frac{\Omega_p}{\sqrt{\Omega_p^2+\Omega_{C2}^2}}|4\rangle$, and $|D_3\rangle = \frac{\Omega_{C2}}{\sqrt{\Omega_{C1}^2+\Omega_{C2}^2}}|2\rangle + \frac{\Omega_{C1}}{\sqrt{\Omega_{C1}^2+\Omega_{C2}^2}}|4\rangle$, The total dark state is superposition of those three dark states. The third dark state $|D_3\rangle$ should be viewed as the production of interaction between two dark resonances; it means the absorption spectrum (enhanced EIT dip) contains the interference term when the double dark resonances are tuned to be degenerate. In other words, the enhancement of EIT dip and susceptibility is the result of quantum interference rather than simple incoherent sum of the degenerate dark resonances. The similar behavior has also been observed in the tripod-type system [32].

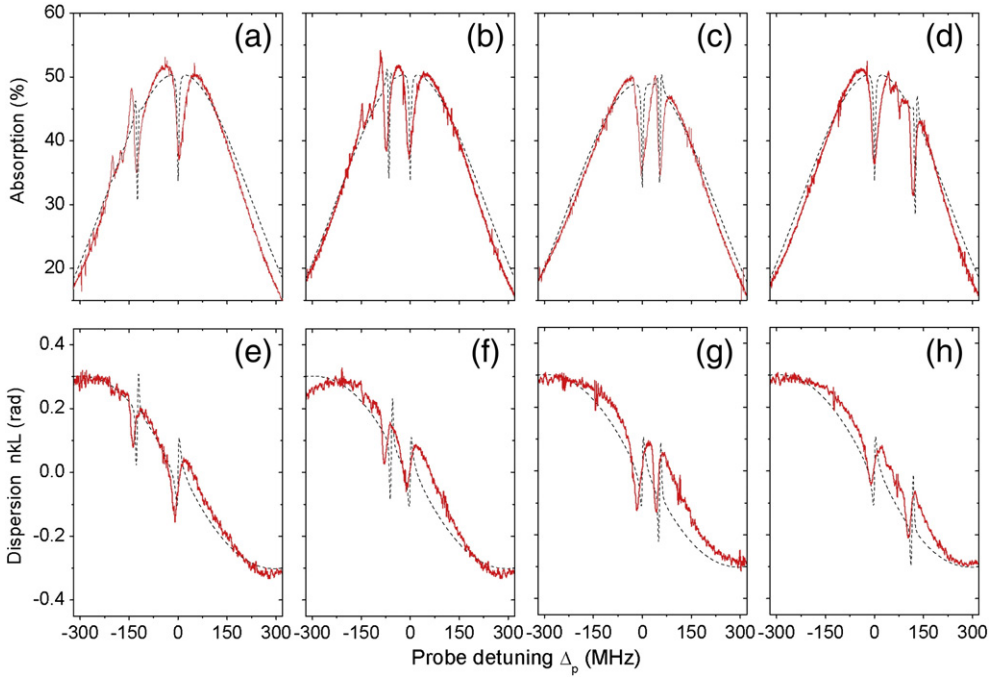

Fig. 4. Red solid curves, experimental measured absorption [(a)–(d)] and the corresponding dispersion [(e)–(h)] as a function of probe detuning Δ_p. Black dashed curves, theoretical predictions calculated with parameters $\Delta_{C1}=0$ MHz, (a) $\Delta_{C2}=130$ MHz; (b) $\Delta_{C2}=60$ MHz; (c) $\Delta_{C2}=-60$ MHz; (d) $\Delta_{C2}=-130$ MHz; other parameters are the same as in Fig. 3 (c).

The dashed curves in Fig. 3 are the corresponding theoretical calculations of the probe absorption and dispersion versus probe detuning. The spontaneous decay rate $\Gamma_{31}=\Gamma_{32}=3.0$ MHz, $\Gamma_{43}=0.4$ MHz, the nonradiative decay rate between two ground level is $\Gamma_{31}=0.1$ MHz. The experimental results are in good agreement with the theoretical simulations, but there are still small differences between them, it is mainly because of three reasons. First, there are effects induced by the levels ^{87}Rb $5D_{3/2}$, $F=2, 3$ shown as the circled section of Fig. 3 (c) and (h). As a matter of fact, the observed EIT spectra can be simulated by adding the contributions due to each of these closely lying hyperfine levels ($F=1$, 2); this kind of phenomenon has been investigated by Badger et al. [33]. Second, we consider only a simple four-level system, ignoring the magnetic sublevels that might make some small changes to the line shape. Third, the system is not closed. The upper level $5D_{3/2}$ decays to other levels such as $5P_{3/2}$, $6P_{1/2}$, and $6P_{3/2}$.

After studying EIT at the exact resonant conditions of the two coupling fields with atomic transition frequencies, we next study how these detunings bring changes in the dark resonances of the system. If the first coupling field detuning is kept at $\Delta_{C1}=0$ MHz and the second coupling field is detuned from positive to negative ($\Delta_{C2}=130$, 60, -60 and -130 MHz), then there is a shift in the EIT window (dark resonance) of the ladder sub-system, as shown in Fig. 4. On the other hand, Fig. 5 shows the situation that the second coupling field detuning is kept at resonance $\Delta_{C2}=0$ MHz and the first coupling field is detuned from negative to positive ($\Delta_{C2}=-130$, -60, 60 and 130 MHz). Figs. 4 and 5 imply that one can effectively modulate the shape and location of one EIT window while keeping the other one unchanged by controlling the detunings of the coupling fields—something difficult to achieve with one of the sub-systems alone. The double dark resonances characteristic in a four-level tripod system has been experimentally demonstrated, and an absorptive resonance with sub-natural line-width is observed by applying a magnetic field [34]. The width of EIT windows in the inverted-Y and tripod configuration system are both mainly affected by the Rabi frequency of corresponding coupling fields. While the dark state in the inverted-Y system usually contains the exciting state, so decoherence in the inverted-Y system is more larger than that in the tripod system, and larger decoherence means more residual absorption in the EIT window [1].

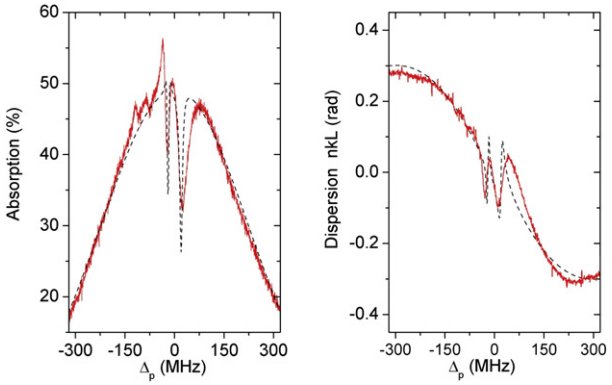

Fig. 6. Red solid curves, experimental measured absorption and the corresponding dispersion as a function of probe detuning Δ_p. Black dashed curves, theoretical predictions calculated with parameters $\Delta_{C1}=\Delta_{C2}=20$ MHz; other parameters are the same as in Fig. 3 (c).

Fig. 6 describes the absorption and dispersion properties for $\Delta_{C1}=\Delta_{C2}=20$ MHz, two EIT windows symmetrically appear in the vicinity of the probe resonance transition, separated by a sharp absorption peak. In this situation, we can calculate the change in dispersion over frequency at the center of two EIT windows, which yield the group refractive indexes $n_{p1}=6.33$ and $n_{p2}=7.58$ due to the atomic coherence induced by coupling fields Ω_{C1} and Ω_{C2}, respectively. By manipulating the intensity of the two coupling fields, the group velocity in two EIT channels can be controlled independently.

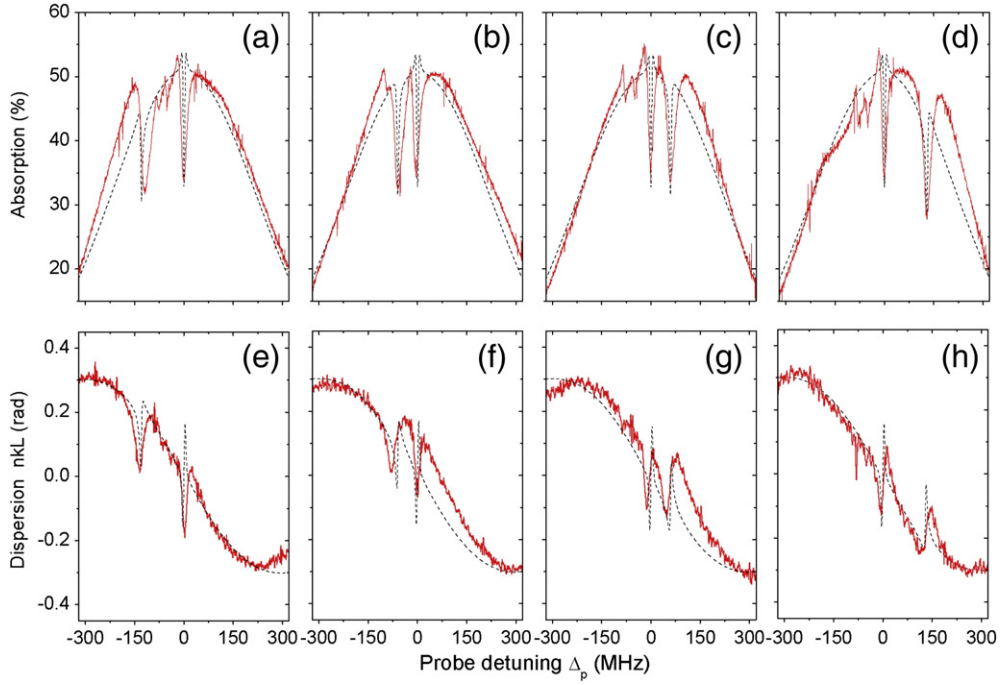

Fig. 5. Red solid curves, experimental measured absorption [(a)–(d)] and the corresponding dispersion [(e)–(h)] as a function of probe detuning Δ_p. Black dashed curves, theoretical predictions calculated with parameters $\Delta_{C2}=0$ MHz, (a) $\Delta_{C1}=-130$ MHz; (b) $\Delta_{C1}=-60$ MHz; (c) $\Delta_{C1}=60$ MHz; (d) $\Delta_{C1}=130$ MHz; other parameters are the same as in Fig. 3 (c).

The two dark resonances emerging in a single transition spectral line may be used as two adjacent information channels in quantum communication, where the weak light carriers can have ultra-slow group velocities due to the steep dispersion. The corresponding theoretical calculations of the probe absorption and dispersion properties are also plotted in dashed curves in above figures. The experimental measured EIT dips are not very deep, the residual absorption is mainly caused by the atomic collisions and inhomogeneous broadening due to Doppler effect, as well as the linewidths of lasers and the divergence among them. For the purpose of observing better phenomena, one can get phase-coherent lasers separated in frequency by the ground-state hyperfine splitting. And the laser linewidths can be suppressed by feedback locking and phase locking the lasers used in the experiment.

4. Conclusions

We have studied the phenomenon of EIT and its dispersion properties in a four-level inverted-Y atomic system. Such a system can be considered to be composed of a three-level ladder-type system and a three-level Λ-type system. The dark resonances of both sub-systems due to the atomic coherence induced by the two coupling fields persist in this four-level system without mutually destroying each other. By manipulating the system parameters it is possible to control the double dark resonances to be separate or degenerate, companied with corresponding dispersion properties. The properties of these dark resonances can be manipulated to design a desired atomic response, and the dispersion control technique can find important applications in two-channel quantum communication and information storage.

Acknowledgements

The authors acknowledge the financial support from the NSFC (Grant No. 10774059, 11074097, 10904048), the National Basic Research Program (Grant No. 2006CB921103, 2011CB921603) of P.R. China, and the Graduate Innovation Fund of Jilin University.

References

[1] S.E. Harris, Phys. Today 50 (1997) 36;
M. Fleischhauer, A. Imamoğlu, J.P. Marangos, Rev. Mod. Phys. 77 (2005) 633.
[2] L.V. Hau, S.E. Harris, Z. Dutton, C.H. Behroozi, Nature 397 (1999) 594, (London).
[3] M.M. Kash, V.A. Sautenkov, A.S. Zibrov, L. Hollberg, G.R. Welch, M.D. Lukin, Y. Rostovtsev, E.S. Fry, M.O. Scully, Phys. Rev. Lett. 82 (1999) 5229.
[4] C. Liu, Z. Dutton, C.H. Behroozi, L.V. Hau, Nature 409 (2001) 490, (London).
[5] D.F. Phillips, A. Fleischhauer, A. Mair, R.L. Walsworth, Phys. Rev. Lett. 86 (2001) 783.
[6] A.V. Turukhin, V.S. Sudarhanam, M.S. Shahriar, J.A. Musser, B.S. Ham, P.R. Hemmer, Phys. Rev. Lett. 88 (2002) 023602.
[7] M. Jain, H. Xia, G.Y. Yin, A.J. Merriam, S.E. Harris, Phys. Rev. Lett. 77 (1996) 4326.
[8] A.J. Merriam, S.J. Sharpe, M. Shverdin, D. Manuszak, G.Y. Yin, S.E. Harris, Phys. Rev. Lett. 84 (2000) 5308.
[9] M.D. Lukin, S.F. Yelin, M. Fleischhauer, M.O. Scully, Phys. Rev. A 60 (1999) 3225.
[10] P. Dong, A.K. Popov, S.H. Tang, J.-Y. Gao, Opt. Commun. 188 (2001) 99.
[11] C.Y. Ye, A.S. Zibrov, Yu.V. Rostovtsev, M.O. Scully, Phys. Rev. A 65 (2002) 043805.
[12] C. Goren, A.D. Wilson-Gordon, M. Rosenbluh, H. Friedmann, Phys. Rev. A 69 (2004) 063802.
[13] L.B. Kong, X.H. Tu, J. Wang, Y. Zhu, M.S. Zhan, Opt. Commun. 269 (2007) 362.
[14] X.G. Wei, J.H. Wu, H.H. Wang, A.J. Li, Z.H. Kang, Y. Jiang, J.Y. Gao, Europhys. Lett. 78 (2007) 44002.
[15] Y. Chen, Y. Liao, H. Chiu, J. Su, I. Yu, Phys. Rev. A 64 (2001) 053806.
[16] S.F. Yelin, V.A. Sautenkov, M.M. Kash, G.R. Welch, M.D. Lukin, Phys. Rev. A 68 (2003) 063801.
[17] L. Yang, L. Zhang, X. Li, L. Han, G. Fu, N.B. Manson, D. Suter, C. Wei, Phys. Rev. A 72 (2005) 053801.
[18] S.E. Harris, Y. Yamamoto, Phys. Rev. Lett. 81 (1998) 3611.
[19] M. Yan, E.G. Rickey, Y. Zhu, Opt. Lett. 26 (2001) 548.
[20] A.V. Sharypov, A.D. Wilson-Gordon, Opt. Commun. 282 (2009) 3591.
[21] S.J. Li, X.D. Yang, X.M. Cao, C.H. Zhang, C.D. Xie, H. Wang, Phys. Rev. Lett. 101 (2008) 073602.
[22] A. Joshi, M. Xiao, Phys. Lett. A 317 (2003) 370.
[23] A. Joshi, M. Xiao, Phys. Rev. A 72 (2005) 062319.
[24] A. Joshi, M. Xiao, Phys. Rev. A 71 (2005), 041801(R).
[25] J.M. Wen, S.W. Du, Y.P. Zhang, M. Xiao, M.H. Rubin, Phys. Rev. A 77 (2008) 033816.
[26] D. Han, Y. Zeng, Y. Bai, W. Chen, H. Cao, H. Lu, C. Huang, L. Chen, Appl. Phys. B 91 (2008) 359.
[27] L.G. Si, W.X. Yang, X.Y. Lü, J.H. Li, X.X. Yang, Eur. Phys. J. D 55 (2009) 161.
[28] M. Yan, E.G. Rickey, Y. Zhu, Phys. Rev. A 64 (2001) 043807.
[29] A.K. Mohapatra, T.R. Jackson, C.S. Adams, Phys. Rev. Lett. 98 (2007) 113003.
[30] M. Xiao, Y. Li, S. Jin, J. Gea-Banacloche, Phys. Rev. Lett. 74 (1995) 666.
[31] U. Khadka, Y.P. Zhang, M. Xiao, Phys. Rev. A 81 (2010) 023830.
[32] S.J. Li, X.D. Yang, X.M. Cao, C.D. Xie, H. Wang, J. Phys. B 40 (2007) 3211.
[33] S.D. Badger, I.G. Hughes, C.S. Adams, J. Phys. B 34 (2001) L749.
[34] N. Gavra, M. Rosenbluh, T. Zigdon, A.D. Wilson-Gordon, H. Friedmann, Opt. Commun. 280 (2007) 374.